

Characterizing Link Connectivity for Opportunistic Mobile Networking: Does Mobility Suffice?

Chul-Ho Lee

Jaewook Kwak

Do Young Eun

Abstract—With recent drastic growth in the number of users carrying smart mobile devices, it is not hard to envision opportunistic ad-hoc communications taking place with such devices carried by humans. This leads to, however, a new challenge to the conventional link-level metrics, solely defined based on user mobility, such as inter-contact time, since there are many constraints including limited battery power that prevent the wireless interface of each user from being always ‘on’ for communication. By taking into account the process of each user’s availability jointly with mobility-induced contact/inter-contact process, we investigate how each of them affects the link-level connectivity depending on their relative operating time scales. We then identify three distinct regimes in each of which (1) the so-called impact of mobility on network performance prevails; (2) such impact of mobility disappears or its extent is not that significant; (3) the user availability process becomes dominant. Our findings not only caution that mobility alone is not sufficient to characterize the link-level dynamics, which in turn can lead to highly misleading results, but also suggest the presence of many uncharted research territories for further exploration.

I. INTRODUCTION

Smart mobile devices such as smartphones and tablets have become commodities in most developed countries with an explosive growth in the number of users and their need for Internet connectivity. Such widespread popularity and the users’ ever-increasing demand for more bandwidth has, however, imposed a serious challenge as the increase in infrastructure capacity does not scale accordingly. To mitigate this asymmetry in the usage of network resources, it is not only interesting but also imperative to examine how opportunistic ad-hoc communications can co-exist and be beneficial with abundant smart mobile devices, as the absence of killer applications and viable/non-disruptive deployment plan is deemed to be the most critical problem of the currently prevalent literature with mobile ad-hoc networks (MANETs) and delay/disruption tolerant networks (DTNs).

As positive signs and prospects for such a direction, several recent studies show that opportunistic information sharing, which is done in a peer-to-peer fashion via WiFi or Bluetooth, can lead to the increase of network capacity/coverage [12], [19], [29], the efficient usage of scarce radio spectrum [35], and mobile data offloading* [17] that is complementary to cellular traffic offloading via femtocell and WiFi. Beside, with multiple interfaces of (smart) mobile devices including cellular, WiFi, and Bluetooth interfaces, there have been a number

of research works on the design of an integrated architecture with cellular and opportunistic ad-hoc networks and relevant applications (e.g., [28], [30]). Despite the active research efforts for opportunistic mobile networking, we reveal, in this paper, that important *but often overlooked* constraints pose a new challenge to the fundamental *link-level* metrics common in the literature and rather make them *problematic*, especially when opportunistic ad-hoc communications take place with smart mobile devices carried by human.

A. Motivation

The prevalent assumption of opportunistic ad-hoc communications in the literature is that any two of mobile nodes can exploit “contact opportunities” based on their geographical proximity. As long as two nodes are close enough to communicate with each other or able to communicate with high SINR, we often say that they are in “contact”, though it depends on the underlying forwarding algorithm whether to utilize the contact opportunity for data transfer. This has been precisely the way the contact duration and the inter-contact time are defined and empirically measured from real traces [11], [20], [13] as well as from synthetic mobility models [9], [10], [27], [24]. Also, the performance of most forwarding/routing algorithms [34], [16], [5], [33], [18], [19] are all evaluated under this hypothesis on the contact opportunities.

However, this implies that each mobile node has to carry a “special” communication device tailored (and also dedicated) to opportunistic ad-hoc communications, which is not the case for smartphones. Clearly, not all the humans carrying smart mobile devices are such “dedicated participants”. More importantly, the basic premise that the “link” for communication is considered to be *available* solely based on nodes’ positions via their mobility, is simply *not true*. First, those devices are known to be power-hungry. One of the biggest concerns for smartphone users is battery lifetime, as their increasing energy demands are far outpacing improvements in battery technology [2]. In this regard, reducing WiFi power consumption – one primary source of battery drainage, has been an active research area for many years,[†] via enhancing the standard WiFi power save mode or a new WiFi duty cycling scheme putting the WiFi radio in the sleep mode for a longer time span (see, e.g., [26] and references therein), although their focus is more on single-hop communication (or direct Internet access) through WiFi. In smartphones, a

The authors are with Department of Electrical and Computer Engineering, North Carolina State University, Raleigh, NC 27695-7911. Email: {clee4, jkwak, dyeun}@ncsu.edu. This work was supported in part by National Science Foundation under grants CNS-0831825 and CCF-0830680.

*This is to reduce the burden on 3G/4G network from high traffic demands.

[†]WiFi is often the preferred way for opportunistic ad-hoc communication due to its higher data rate and longer transmission range, and also simpler peering/service detection procedure, when compared with Bluetooth [17].

low battery can easily deny a link that would otherwise be available. Second, when the WiFi interface is used for Internet access, it is unavailable for other peering users with smartphones via WiFi. Third, such devices are subject to the (time-varying) behavior of each user in cooperation with other users for opportunistic communications. Finally, there are other issues such as lack of incentives to participate, privacy [17], neighbor/device discovery [36], [7], and possible failures/delay to setup connections (or links) [29].

B. Our contributions

Thus motivated, in this paper, we investigate the characteristics of link-level connectivity by taking into account the process of each user’s availability for communication over time (simply, user availability process) in addition to the mobility-induced contact/inter-contact process. We make the following contributions.

- First, we introduce a framework for the link formation process between two mobile nodes to evaluate the actual ‘off-duration’ of the link – the time duration between two successive transfer (not contact) opportunities for the pair, called inter-transfer time, as well as the actual ‘on-duration’ of the link, called transfer-time. We then provide exact formulas for the transfer-time distribution and the mean inter-transfer time. We also show the presence of invariance property for mean transfer/inter-transfer time.
- Second, we investigate how the distributional shape of the inter-transfer time (corresponding to the conventional notion of the inter-contact time) changes while varying the relative time scale between the user availability and contact/inter-contact processes. We identify three distinct regimes in each of which (1) the contact/inter-contact process (or mobility) primarily governs network performance; (2) the impact of mobility on the performance becomes vanishingly small or its extent is not that large as commonly expected; (3) the user availability process becomes dominant. In particular, in the second regime, the inter-transfer time distribution can become arbitrarily close to an exponential, even when the underlying contact/inter-contact dynamics is non-Poisson. However, in the third regime, even when the original inter-contact time is exponentially distributed, the resulting inter-transfer time can significantly deviate from the exponential.
- Finally, we provide extensive simulation results to support our findings. The simulation results are obtained with different user availability processes under various mobility patterns, ranging from a class of random walk models including Lévy walk model to a map-based mobility model with a geographical constraint (Helsinki downtown area) as well as real GPS mobility traces. Our results collectively assert that mobility alone does not suffice to characterize the link-level connectivity and there exists another equally important dimension – ‘user availability’ for communication, that has been largely overlooked in the literature, but is necessary, together with mobility, to correctly understand the link-level dynamics and its resulting network performance.

II. PRELIMINARIES

To set the stage for subsequent exposition, we here first revisit the conventional usage of the link-level metrics in all the mobility-based research and provide related works on mobility-induced performance analysis in the current MANET/DTN literature. We then describe our general reference model for the constituents of the actual link metrics.

A. Link-level metrics in the current literature

Consider two mobile nodes A and B , each of which follows some mobility model in a common domain Ω . Let $A(t), B(t) \in \Omega$ be the position of nodes A and B at time t , respectively. Let $\mathcal{C}_A(t) \subset \Omega$ be the *contact set* (or neighborhood) of node A at time t , i.e., node B can communicate with A at time t if and only if $B(t) \in \mathcal{C}_A(t)$. The simplest and most popular model for communication is the so-called Boolean model, in which the contact set becomes [9], [10], [25]

$$\mathcal{C}_A(t) = \{x \in \Omega : \|x - A(t)\| \leq d\}, \quad (1)$$

where d is some communication/sensing range. Similarly, we can define $\mathcal{C}_B(t)$ under SINR model [10]. Then, the *inter-contact time* of nodes A and B has been defined by

$$T_I \triangleq \inf\{t > 0 : B(t) \in \mathcal{C}_A(t)\}, \quad (2)$$

given that $B(0^-) \in \mathcal{C}_A(0^-)$ and $B(0) \notin \mathcal{C}_A(0)$. In words, the inter-contact time between two nodes is the duration of time these two nodes stay ‘out of contact’ before getting in contact with each other. Similarly, if we replace $\mathcal{C}_A(t)$ in (2) by $\overline{\mathcal{C}}_A(t) = \Omega \setminus \mathcal{C}_A(t)$, we obtain the *contact time* T_C (or contact duration) of A and B .

B. The status quo for mobility-induced link-level dynamics

The inter-contact time has been considered as a key factor for the performance measure in MANETs/DTNs leveraging node mobility toward efficient communications. In particular, Poisson contact assumption[‡] has been prevalent and is still popular in most analytical studies ranging from the capacity-delay tradeoff to the cost-delay tradeoff as well as the analysis and design of forwarding algorithms thanks to its tractable analysis [16], [37], [33], [3], [38]. Only a few works, however, have partially provided empirical and theoretical support on justification for Poisson assumption. As shown in [9] and also empirically observed in [6], Poisson (contact) process arises in a small bounded domain when coupled with a proper time scale of networking operation. Further, there exist a portion of node pairs whose inter-contact time distributions are close to exponential [13].

It is known via a measurement study [20] that the inter-contact time distribution follows a power-law up to a certain characteristic time scale beyond which it decays exponentially fast, which substitutes the argument in [11] that relies upon the power-law *tail* of the inter-contact time distribution. Its mixture behavior thus becomes a critical feature that newly

[‡]Equivalently, the inter-contact time between any pair of mobile nodes is exponentially distributed.

proposed mobility models [27], [24] need to reproduce in order to be more *realistic*, while [20], [9], [10] explain such phenomenon using a class of random walk models. It is also presented in [10], [25] that the network performance under node mobility leading to non-exponential inter-contact time distribution differs substantially from that under Poisson contact assumption. In short, the fundamental basis of Poisson assumption for the vast amount of analytical works in the literature so far is still fragile, while the debate on the ‘true’ characteristics of inter-contact time beyond Poisson regime and its network implication seems unceasing.

C. User availability comes into picture

As seen above, the adoption of link-level metrics based on nodes’ proximity via Boolean (or SINR) model has been prevalent, generating abundant research works in the literature so far. However, as noted earlier, not every ‘contact’ between mobile nodes leads to actual formation of a link. For two mobile nodes to have a chance to communicate, not only they should be ‘close’ to each other in proximity, but also their wireless interfaces be both ‘on’. To properly capture the notion of on/off wireless interfaces, let $I_A(t), I_B(t)$ be 0–1 valued processes representing the ‘availability’ of nodes (or users) A and B at time t , respectively. Specifically, $I_A(t) = 1$ if A is available for opportunistic communication (e.g., its wireless interface is ‘on’ or performing idle listening); and $I_A(t) = 0$ if otherwise. Also, let $A_{\text{on}}, A_{\text{off}}$ be random variables to denote ‘on’ durations (1-period lengths) and ‘off’ durations (0-period lengths) for the availability of node A , respectively. Similarly for $I_B(t), B_{\text{on}}$, and B_{off} . See Figure 1 for illustration.

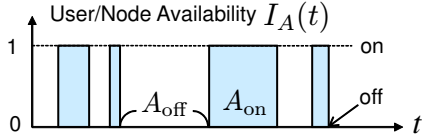


Fig. 1. 0–1 valued process for user availability.

In this setup, the notion of contact set in (1) should be revised accordingly. For a given A – B pair, we say that they have a link, or event $L(A-B)$ occurs, at time t if and only if all the following three conditions are satisfied:

$$(i) B(t) \in \mathcal{C}_A(t), (ii) I_A(t) = 1, \text{ and } (iii) I_B(t) = 1. \quad (3)$$

Thus, the link formation process between A and B is yet another 0–1 valued process, given by the indicator function of the event $L(A-B)$ at time t . To be precise,

$$\mathbf{1}_{\{L(A-B)\}}(t) = \mathbf{1}_{\{B(t) \in \mathcal{C}_A(t)\}} \cdot I_A(t) \cdot I_B(t), \quad (4)$$

and the notion of the inter-contact time between A and B can be generalized into the following:

$$L_{\text{off}} \triangleq \inf\{t > 0 : \mathbf{1}_{\{L(A-B)\}}(t) = 1\}, \quad (5)$$

given that $\mathbf{1}_{\{L(A-B)\}}(0^-) = 1$ and $\mathbf{1}_{\{L(A-B)\}}(0) = 0$, which we call *inter-transfer time* for the A – B pair. In words, it is the ‘off’ duration of the process $\mathbf{1}_{\{L(A-B)\}}(t)$. Again, if we

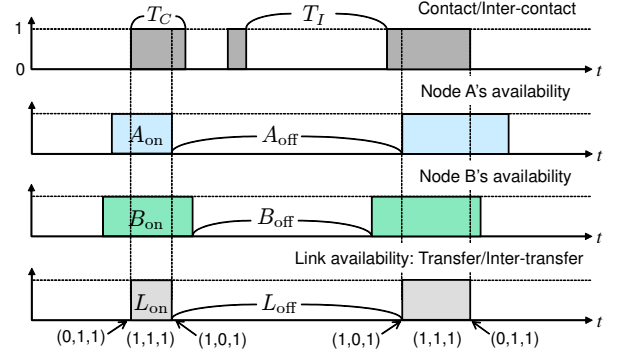


Fig. 2. Link formation process for A – B pair

similarly replace $\mathbf{1}_{\{L(A-B)\}}(t) = 1$ in (5) by $\mathbf{1}_{\{L(A-B)\}}(t) = 0$ (with properly reversed conditional event), then we obtain the *transfer time* L_{on} (or the link ‘on’ duration) for the A – B pair. Figure 2 depicts the link formation process between A and B with its resulting transfer/inter-transfer time.

In summary, the actual link formation dynamics should be described by jointly considering users’ mobility and their availability processes together. While the conventional usage of contact-based metrics is *only* valid for the scenario with all ‘dedicated’ users for communication, our link definitions correctly capture both users’ mobility and availability, and are general enough to cover a wide range of scenarios that take into account all the constraints (including limited batter power) affecting the link formation dynamics.

III. ANALYSIS OF LINK-LEVEL DYNAMICS

A. Transfer-time distribution and mean inter-transfer time

We first provide exact formulas for the transfer-time distribution $\mathbb{P}\{L_{\text{on}} > t\}$ and the mean inter-transfer time $\mathbb{E}\{L_{\text{off}}\}$, in terms of distributions of contact/inter-contact time and on/off duration in the user availability. To proceed, we consider the superposition of three on/off processes that appear in the definition of link indicator as in (4). We assume that these on/off processes are independent of each other and the process $Z(t) \triangleq (\mathbf{1}_{\{B(t) \in \mathcal{C}_A(t)\}}, I_A(t), I_B(t)) \in \{0, 1\}^3$ is stationary, ergodic, and right-continuous such that its state transitions occur at distinct time instants (and so is each of three 0–1 valued processes). Here, a state transition means the change of *any one* element (but not multiple elements) of the 3-dimensional vector, as $Z(t)$ is the superposed process. For example, transition from $(0, 0, 0)$ to $(1, 1, 1)$ occurs only with probability zero. Note that $\mathbf{1}_{\{L(A-B)\}}(t) \equiv \mathbf{1}_{\{Z(t) = (1, 1, 1)\}}$. Then, from stationarity, we have

$$P_C \triangleq \mathbb{P}\{\mathbf{1}_{\{B(t) \in \mathcal{C}_A(t)\}} = 1\} = \frac{\mathbb{E}\{T_C\}}{\mathbb{E}\{T_C\} + \mathbb{E}\{T_I\}}.$$

Similarly for $P_A \triangleq \mathbb{P}\{I_A(t) = 1\}$ and $P_B \triangleq \mathbb{P}\{I_B(t) = 1\}$. Also, from independence, we have

$$\mathbb{P}\{Z(t) = (1, 1, 1)\} = P_C P_A P_B = \frac{\mathbb{E}\{L_{\text{on}}\}}{\mathbb{E}\{L_{\text{on}}\} + \mathbb{E}\{L_{\text{off}}\}}, \quad (6)$$

where the last equality is from $\mathbb{P}\{Z(t) = (1, 1, 1)\} = \mathbb{P}\{\mathbf{1}_{\{L(A-B)\}}(t) = 1\}$ and stationarity. To avoid triviality, we

assume that $P_C, P_A, P_B \in (0, 1)$. If any one of these 0–1 valued processes is always one over time t , then we can simply ignore the process in evaluating the link formation dynamics. Also, if there is a process giving zero for all t , then the link for the A – B pair is never formed over t .

In addition, we define by T_C^e the residual (or remaining) contact time from a random time instant when A and B are in contact, whose distribution is given by

$$\mathbb{P}\{T_C^e > t\} = \frac{1}{\mathbb{E}\{T_C\}} \int_t^\infty \mathbb{P}\{T_C > s\} ds.$$

This is often called the *equilibrium* distribution of T_C . Similarly, we can define by $T_I^e, A_{\text{on}}^e, A_{\text{off}}^e, B_{\text{on}}^e,$ and B_{off}^e the residual time for $T_I, A_{\text{on}}, A_{\text{off}}, B_{\text{on}},$ and $B_{\text{off}},$ respectively. Then, we have the following.

Theorem 1: The transfer-time distribution is

$$\begin{aligned} \mathbb{P}\{L_{\text{on}} > t\} = \tau \cdot & \left[\frac{\mathbb{P}\{T_C > t\}}{\mathbb{E}\{T_C\}} \mathbb{P}\{A_{\text{on}}^e > t\} \mathbb{P}\{B_{\text{on}}^e > t\} \right. \\ & + \frac{\mathbb{P}\{A_{\text{on}} > t\}}{\mathbb{E}\{A_{\text{on}}\}} \mathbb{P}\{T_C^e > t\} \mathbb{P}\{B_{\text{on}}^e > t\} \\ & \left. + \frac{\mathbb{P}\{B_{\text{on}} > t\}}{\mathbb{E}\{B_{\text{on}}\}} \mathbb{P}\{T_C^e > t\} \mathbb{P}\{A_{\text{on}}^e > t\} \right] \quad (7) \end{aligned}$$

with $\tau \triangleq \mathbb{E}\{L_{\text{on}}\} = [1/\mathbb{E}\{T_C\} + 1/\mathbb{E}\{A_{\text{on}}\} + 1/\mathbb{E}\{B_{\text{on}}\}]^{-1}$. Also, the mean inter-transfer time is given by $\mathbb{E}\{L_{\text{off}}\} = \tau \cdot [1/(P_C P_A P_B) - 1]$. \square

Theorem 1 is a reinterpretation of Theorem A.1 in [23] under our setting whose proof is built upon Palm calculus and is a consequence of Formula (1.4.5) in [4]. It is worth noting that Theorem 1 does not require any distributional or independence assumption on the joint distribution of the *successive* contact and inter-contact times (resp. on and off durations) for the contact process (resp. user availability process).

While we refer to [23] for the rigorous proof (see also [4] for more in-depth mathematical treatment of Palm calculus), we here briefly explain the principle behind the Palm calculus in obtaining the transfer-time distribution $\mathbb{P}\{L_{\text{on}} > t\}$ in (7). In essence, the Palm probability of an event is the conditional probability, given that a point of some specific point process occurs at the origin $t = 0$. Define a subset $S \triangleq \{(0, 1, 1), (1, 0, 1), (1, 1, 0)\}$. Then, recall that the transfer time L_{on} is nothing but the first passage time to the event $\{\mathbf{1}_{\{L(A-B)\}}(t) = 0\}$, given that $\mathbf{1}_{\{L(A-B)\}}(0^-) = 0$ and $\mathbf{1}_{\{L(A-B)\}}(0) = 1$. Or, equivalently, it is the first passage time to $\{Z(t) \in S\}$ given that $Z(0^-) \in S$ and $Z(0) = (1, 1, 1)$, as depicted in Figure 2 (bottom). For the superposed process $\mathbf{1}_{\{Z(t)=(1,1,1)\}}$, the Palm calculus framework enables to identify such conditional event as a transition point, with the transition from $s \in S$ to $(1, 1, 1)$ occurring at $t = 0$, and evaluate the time until when transition from $(1, 1, 1)$ to $s' \in S$ takes place. For instance, if $Z(0^-) = (0, 1, 1)$ and $Z(0) = (1, 1, 1)$, from independence, it follows that

$$\mathbb{P}\{L_{\text{on}} > t\} = \mathbb{P}\{T_C > t\} \mathbb{P}\{A_{\text{on}}^e > t\} \mathbb{P}\{B_{\text{on}}^e > t\},$$

where the residual times A_{on}^e and B_{on}^e are used instead of A_{on} and B_{on} since $I_A(0^-) = 1$ and $I_B(0^-) = 1$. (See also the first

part of Figure 2.) This transition from $Z(0^-) = (0, 1, 1)$ to $Z(0) = (1, 1, 1)$, among three possible transitions from $s \in S$ to $(1, 1, 1)$, occurs with probability proportional to $1/\mathbb{E}\{T_C\}$. Similarly for the other two possible transitions. Thus, we have (7) with normalizing constant τ to ensure that $\mathbb{P}\{L_{\text{on}} > 0\} = 1$.

In contrast to the transfer time, the inter-transfer time can, however, span over infinitely many transition points (e.g., $(1, 1, 1) \rightarrow (1, 1, 0) \rightarrow \dots \rightarrow (1, 0, 1) \rightarrow (1, 1, 1)$) of the process $\mathbf{1}_{\{Z(t)=(1,1,1)\}}$, which in turn prevents obtaining the inter-transfer time distribution in any useful form. Nonetheless, the *mean* inter-transfer time $\mathbb{E}\{L_{\text{off}}\}$ can still be obtained in terms of the mean transfer time $\mathbb{E}\{L_{\text{on}}\}$ using the identity in (6).

Invariance principle: Theorem 1 says that the mean transfer/inter-transfer time is solely determined by the mean contact/inter-contact time and the mean on/off duration for each node's availability. Also, it was shown in [10] that the mean contact/inter-contact time is invariant under a class of random walk models whose stationary distributions are uniform but with varying temporal dynamics (the degree of motion correlation). Thus, by Theorem 1, such *invariance property* is still preserved for the transfer/inter-transfer time under the same class of mobility models and various distributions of on/off duration for user availability, as long as their mean values remain the same.

Nonetheless, as seen from the folklore about the impact of different mobility patterns on network performance, the inter-transfer time L_{off} (corresponding to the conventional notion of inter-contact time) would still be a critical factor governing the network performance, while its mean value (first-order) is *insufficient* to predict the performance. Thus, in the following section, we will investigate the distributional shape of the inter-transfer time to better understand its higher-order behaviors.

B. Inter-transfer time distribution

While it is impossible to obtain the exact form of the inter-transfer time distribution, we here present how the *shape* of the distribution changes according to different relative time scales between contact/inter-contact dynamics and user availability dynamics, and explain its impact on network performance.

To this end, we consider that the contact/inter-contact process for the A – B pair is an alternating renewal process, i.e., the (successive) inter-contact times of the pair are *i.i.d.* and their contact-times are also *i.i.d.* It is known that the contact time between two nodes is much smaller than their inter-contact time and thus the contact duration is often ignored in the performance analysis of many forwarding/routing algorithms [11], [16], [37], [33], [3], [38]. This implies that the stationary probability that nodes A and B are in contact, or P_C , is very small, and also $\mathbb{E}\{T_C\} \ll \mathbb{E}\{T_I\}$. We also note that the inter-contact time distribution is typically a mixture of power-law and exponential functions [9], [20], [10], and utilize the following.

Lemma 1: [15] For any completely monotone function $g : \mathbb{R}_+ \rightarrow \mathbb{R}_+$, i.e., $(-1)^n g^{(n)}(t) \geq 0$ for all $t > 0$ and $n = 0, 1, \dots$, where $g^{(n)}$ is the n^{th} derivative of g , there exists a non-negative function $h(s)$ such that $g(t) = \int_0^\infty e^{-st} h(s) ds$. \square

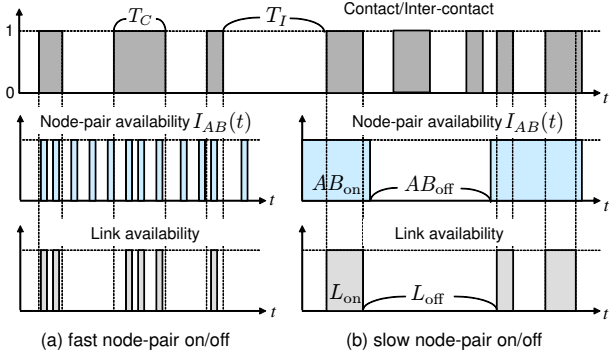


Fig. 3. Examples of user-pair on/off dynamics over (a) faster time scale, and (b) slower time scale, than that of contact/inter-contact dynamics.

In words, a completely monotone function is a (generalized) mixture of exponential functions. Note that both power-law and exponential functions are completely monotone, and so is their mixture. It follows that the ccdf of the inter-contact time T_I showing ‘dichotomic’ behavior (first power-law followed by exponential) in [20], [10] is also completely monotone. In addition, it was presented in [14] that a *finite* mixture of exponential distributions (completely monotone) can approximate a long-tail (or power-law) distribution over a wide range of interest, when the tail of the approximated distribution eventually decays exponentially fast. We thus consider T_I with completely monotone density (or ccdf) having finite moments.

For simplicity and uncluttered exposition, from now on, we consider the user-pair availability for communication rather than considering the availability of users A and B separately. Specifically, let $I_{AB}(t) = I_A(t)I_B(t)$, indicating whether or not *both* A and B are ‘on’ or available for communication (regardless of their geographical proximity). Similarly as before, let AB_{on} and AB_{off} be the random variables denoting ‘on’ duration (1-period length) and ‘off’ duration (0-period length) for the process $I_{AB}(t)$, respectively. We assume that this process is also an alternating renewal process. Clearly, the stationary probability that both nodes A and B are available for communication, say P_{AB} , is $P_{AB} = \mathbb{E}\{AB_{\text{on}}\} / (\mathbb{E}\{AB_{\text{on}}\} + \mathbb{E}\{AB_{\text{off}}\}) = P_A P_B$. As there are many factors that prevent the wireless interface of each user from being always ‘on’ for communication, we focus on the case that P_{AB} is small.

We next identify the distributional *shape* of the inter-transfer time L_{off} (or the actual off-duration of the link) depending on how quickly the node-pair on/off dynamics changes as compared with the contact/inter-contact dynamics, while P_{AB} remains fixed.

Fast node-pair on/off dynamics: The A – B pair becomes on/off for communication on a (fast) time scale, faster than the contact/inter-contact time dynamics, as shown in Figure 3(a). This regime includes the case that $AB_{\text{on}} + AB_{\text{off}} < T_C$ and $AB_{\text{on}} + AB_{\text{off}} < T_I$ with high probability. In this regime, most samples of T_I will appear almost ‘as is’ in L_{off} samples, while there are some newly created small-valued L_{off} samples coming from the small-valued AB_{off} . Thus, the distribution of L_{off} is largely determined by that of T_I , i.e., the usual notion of ‘impact of mobility’ prevails. In other words, almost all

contact opportunities can translate into “transfer” opportunities. One extreme example in this regime would be the usual measurement scenario to collect contact traces with ‘always-on’ communication devices whose sensing interval (or the granularity of the experiment) is relatively small such that almost every contact event is properly captured and recorded.

Slow node-pair on/off dynamics: The 0–1 valued $I_{AB}(t)$ process changes very slowly as compared with the contact/inter-contact dynamics, as depicted in Figure 3(b). This regime also includes the case that $T_C + T_I < AB_{\text{on}}$ and $T_C + T_I < AB_{\text{off}}$ with high probability. Then, one can see that the large-valued samples of L_{off} are mostly from AB_{off} , while relatively smaller-valued samples of L_{off} are from T_I . That is,

$$L_{\text{off}} \stackrel{d}{\approx} \begin{cases} T_I & \text{if } T_I < AB_{\text{on}}, \\ AB_{\text{off}} & \text{otherwise.} \end{cases} \quad (8)$$

As an example, suppose the inter-contact time T_I is exponentially distributed with small average value (i.e., the typical Poisson contact model in the literature) and AB_{off} follows some wildly fluctuating distribution (e.g., heavy-tail or dichotomic distribution). Then, even when the mobility-induced contact process is a pure Poisson, we expect that the distribution of the inter-transfer time L_{off} , can significantly deviate from an exponential, as governed by that of AB_{off} .

Intermediate node-pair on/off dynamics: Both node-pair availability process and contact/inter-contact process operate on a similar time scale, and so there is no dominant process between them in deciding the link formation dynamics. This regime is highly non-trivial, but could be relevant in reality. Under this regime, we show, in considerable generality, that the distribution of the inter-transfer time L_{off} becomes very close to an *exponential*, which will also be supported by extensive simulations later on.

We consider that $I_{AB}(t)$ is likely to change at least once over a period of the inter-contact time T_I , while AB_{off} is larger than the contact duration T_C with high probability. Recall that $\mathbb{E}\{T_C\} \ll \mathbb{E}\{T_I\}$, and so this condition can hold for a large range of $AB_{\text{on}}, AB_{\text{off}}$. An example is when $T_C < AB_{\text{on}} < T_I$ and $T_C < AB_{\text{off}} < T_I$ with high probability. Then, the (stationary) probability that the transfer opportunity is granted, or the actual link is established, upon a physical contact, denoted as P_{link} , becomes

$$P_{\text{link}} = P_{AB} + (1 - P_{AB})\mathbb{P}\{T_C > AB_{\text{off}}^e\}, \quad (9)$$

where AB_{off}^e denotes the residual time until when the A – B pair becomes ‘on’ for communication, measured from a random time instant at which the pair is ‘off’. To see this, first note that when a contact opportunity arises, the probability that both A and B are ready for communication is simply the stationary probability that both are ‘on’, or P_{AB} . Also, even if at least one of A and B is *not available* for communication at a physical contact (the beginning of contact duration T_C), both can become available over the course of contact duration T_C , with probability $\mathbb{P}\{T_C > AB_{\text{off}}^e\}$ as shown in (9).

Let T_i ($i = 1, 2, \dots$) be *i.i.d.* copies of T_I . Then, if we ignore the contact duration T_C toward the inter-transfer time L_{off} (recall that T_C is typically much smaller than the inter-contact time T_I and often ignored in the literature), then the inter-transfer time L_{off} can be well approximated by $L_{\text{off}} \stackrel{d}{=} \sum_{i=1}^N T_i$, where N is an independent geometric random variable with parameter P_{link} . This is because the process $I_{AB}(t)$, under the (relative) time scale of interest, does not create dependency over successive contact epochs, implying that the opportunity of the link formation between A and B upon their physical contact with probability P_{link} is mostly independent of their previous/next opportunities. Then, we have the following.

Theorem 2: Under the aforementioned setting with intermediate time scale for node-pair on/off dynamics,

$$\sup_{t>0} \left| \mathbb{P}\{L_{\text{off}} > t\} - e^{-\frac{t}{\mathbb{E}\{L_{\text{off}}\}}} \right| \leq 1 - \frac{2}{P_{\text{link}}(c_{T_I}^2 - 1) + 2},$$

where $c_{T_I}^2 \triangleq \text{Var}\{T_I\}/\mathbb{E}\{T_I\}^2$ is the squared coefficient of variation (CoV) of the inter-contact time T_I . \square

Proof: First, for the inter-contact time T_I with its pdf $f(t)$, consider its ‘failure rate’ $\lambda(t)$ at time t , defined by $\lambda(t) \triangleq f(t)/\mathbb{P}\{T_I > t\}$, i.e., $\lambda(t)dt$ is the probability that two nodes will meet in the interval $(t, t + dt)$, given that they haven’t met until time t . If $\lambda(t)$ is decreasing in t , it is called decreasing failure rate or simply DFR [31]. It is known that a random variable (rv) whose distribution is completely monotone is DFR [31], so is T_I (and also T_i). Since the DFR property is also preserved under geometric compounding, i.e., the sum of a geometrically distributed number of *i.i.d.* DFR rvs is also DFR [32], L_{off} is DFR. Moreover, it was shown in [8] that for a DFR rv Z with $\mathbb{E}\{Z\} < \infty$,

$$\sup_t \left| \mathbb{P}\{Z > t\} - e^{-t/\mathbb{E}\{Z\}} \right| \leq 1 - \frac{2(\mathbb{E}\{Z\})^2}{\mathbb{E}\{Z^2\}} = 1 - \frac{2}{c_Z^2 + 1},$$

where c_Z^2 is the squared CoV of rv Z . After conditioning and some computations, one can observe that

$$c_{L_{\text{off}}}^2 - 1 = P_{\text{link}} \cdot (c_{T_I}^2 - 1).$$

Putting these together, the result follows. \blacksquare

Theorem 2 says the maximum gap between the inter-transfer time distribution and its exponential counterpart can be measured by how close $P_{\text{link}}(c_{T_I}^2 - 1)$ is to zero. Note that $c_{T_I}^2 \geq 1$, as the inter-contact time T_I is DFR [31]. If T_I itself is exponentially distributed with $c_{T_I}^2 = 1$, the upper bound becomes zero. In other words, the exponential behavior of T_I carries over to the inter-transfer time L_{off} . More importantly, even when T_I follows a non-exponential distribution (say, a mixture of power-law and exponential distributions [20], [9]) with $c_{T_I}^2 > 1$, $P_{AB} = P_A P_B$ is typically small valued and under the intermediate time scale of interest for pair on/off dynamics, $\mathbb{P}\{T_C > AB_{\text{off}}\}$ is also small, and so is $\mathbb{P}\{T_C > AB_{\text{off}}^e\}$.[§] All of these make P_{link} in (9) smaller,

[§]When the distribution of AB_{off} is completely monotone (reasonable as for the case of inter-contact time T_I), AB_{off}^e is stochastically larger than AB_{off} , implying that $\mathbb{P}\{T_C > AB_{\text{off}}^e\} < \mathbb{P}\{T_C > AB_{\text{off}}\}$.

suggesting that the difference between the actual distribution of L_{off} and its corresponding exponential distribution becomes negligible over entire t . Therefore, in this regime, we expect that the so-called ‘impact of mobility’ on network performance disappears or its extent not significant.

In summary, for a given contact/inter-contact dynamics and a small, but fixed P_{AB} , our findings imply that the impact of mobility on network performance first prevails when the node-pair on/off dynamics $I_{AB}(t)$ is operating on a relatively faster time scale. Then, such impact becomes vanishingly small as the time scale for $I_{AB}(t)$ starts to grow, but still comparable to that of contact/inter-contact process. However, if the time scale for $I_{AB}(t)$ gets arbitrarily larger (slow pair on/off dynamics), the on/off dynamics for communication availability itself will eventually take over in deciding the network performance.

IV. SIMULATION RESULTS

We provide simulation results using ONE simulator [21] with proper modification and pre-/post-processing to support our findings. We consider an alternating renewal process as the availability process of each user (say, A) for which $\mathbb{P}\{A_{\text{on}} > t\} = e^{-t/\mathbb{E}\{A_{\text{on}}\}}$. We test two different distributions for A_{off} ; (i) exponential $\mathbb{P}\{A_{\text{off}} > t\} = e^{-t/\mathbb{E}\{A_{\text{off}}\}}$ and (ii) hyper-exponential $\mathbb{P}\{A_{\text{off}} > t\} = q_1 e^{-\mu_1 t} + q_2 e^{-\mu_2 t}$, where

$$q_1 = 0.5 \cdot \left[1 - \sqrt{(c_{A_{\text{off}}}^2 - 1)/(c_{A_{\text{off}}}^2 + 1)} \right] = 1 - q_2,$$

$\mu_1 = 2q_1/\mathbb{E}\{A_{\text{off}}\}$, and $\mu_2 = 2q_2/\mathbb{E}\{A_{\text{off}}\}$. We use the same $\mathbb{E}\{A_{\text{off}}\}$ for both cases and set the squared CoV of the hyper-exponential distribution to $c_{A_{\text{off}}}^2 = 16$, to see any impact of more variability of A_{off} around its mean than the exponential counterpart. In all cases, we fix $P_A = \frac{\mathbb{E}\{A_{\text{on}}\}}{\mathbb{E}\{A_{\text{on}}\} + \mathbb{E}\{A_{\text{off}}\}} = 0.1$ to emulate the low chance of communication availability per node (caused by many factors), while varying $\mathbb{E}\{A_{\text{on}}\}$ (and also $\mathbb{E}\{A_{\text{off}}\} = (1/P_A - 1)\mathbb{E}\{A_{\text{on}}\} = 9\mathbb{E}\{A_{\text{on}}\}$) to generate different relative time scales between user availability and mobility-induced contact/inter-contact processes.

Random walk models: We first consider a class of random walk (RW) and random direction (RD) models [16], [37], [9], [10], [25]. In the former, a mobile node follows a randomly chosen direction for some random amount of time – a randomly chosen step-length (or distance) divided by a random node speed, and then chooses another direction and repeat the same process, with reflective boundary condition. We consider constant and exponential step-length distributions with mean 20m, each of which approximates Brownian motion. We also consider power-law distribution for the step-length (say, L), i.e., $\mathbb{P}\{L > l\} = l^{-\alpha}$ defined over $l \geq 1$ with $\alpha \in (0, 2)$, which is known as the *Lévy walk* (LW) model [22]. We here use $\alpha = 1.2$ for the exponent, implying that, theoretically, the step-length has finite mean and infinite variance. In the RD model, a mobile node moves in a randomly chosen direction until to hit the boundary, and then chooses another direction and repeats. In all cases, the initial node locations are drawn from uniform distribution over the domain whose size is $1000\text{m} \times 1000\text{m}$, and the node speed is set to 1 m/s. We use the Boolean

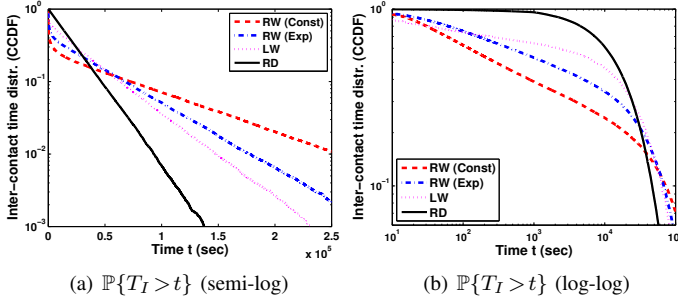


Fig. 4. ccdf of inter-contact time of a given pair in (a) linear-log scale, and (b) log-log scale to clearly show the power-law ‘head’ behavior.

model for contact with transmission range $d = 20\text{m}$, and do not consider the pause of mobile nodes in order to focus on the random mobility pattern itself.

Before going into the details, we measure the distribution of inter-contact time between two mobile nodes, each of which moves according to one of the above models. As seen from Fig. 4, the ccdf of the inter-contact time first follows a power-law then decays exponentially fast later on – the so-called dichotomic distribution [20], [10], for RW models with constant and exponential step-length distributions as well as LW model, while the inter-contact time distribution under RD model is exponential. These are well expected from the existing results [9], [10], [25]. For all of these models, empirical measurements give $\mathbb{E}\{T_I\} \approx 2 \times 10^4$ and $\mathbb{E}\{T_C\} \approx 25$, as also expected from the invariance property in [10] where the mean contact/inter-contact time does not depend on the choice of step-length under the RW models.

For network performance evaluation, we next measure the average message delay of the epidemic routing protocol, a widely used reference protocol regarding opportunistic communications [16], [37], [10], [6], [17]. Here, the total number of nodes in the domain is 100, and each of them independently moves according to one of the aforementioned mobility models. To ensure a fair comparison under different relative time scales between user (or user-pair) availability and mobility-induced contact/inter-contact processes, we evaluate how much the average message delay deviates from the case where every inter-transfer time L_{off} sample is now independently drawn from an exponential distribution with the same mean. This way, we can identify under which regime L_{off} becomes close to an exponential, even when the original T_I is highly non-exponential (dichotomic).

When L_{off} is exponentially distributed for each pair, we can reuse the existing theoretical result for the average delay of epidemic routing protocol [16], [37]

$$\mathbb{E}\{D\} = \frac{1}{\lambda n} \sum_{i=1}^n \frac{1}{i} \approx \frac{1}{\lambda n} \log n, \quad (10)$$

where $n+1$ is the total number of nodes, and mobile nodes make contacts with each other according to a Poisson process with rate λ . Note that in this setup the transfer opportunity is always granted upon encounter. We then use this formula with λ set as $\lambda' = 1/\mathbb{E}\{L_{\text{off}}\}$, where $\mathbb{E}\{L_{\text{off}}\}$ is empirically

measured for each of our simulation settings.[¶]

Figure 5(a) shows the performance ratio of the average delay obtained under each mobility pattern to the analytical prediction by (10), while varying $\mathbb{E}\{A_{\text{on}}\}$ from 1 to 32805, for the case of an exponential off-duration A_{off} . The inset in Figure 5(a) shows the performance ratio when all nodes are always ‘on’ for communication, for which we use $\lambda' = 1/\mathbb{E}\{T_I\}$. We clearly see the impact of mobility on network performance, as these ratios are quite different over different choices of mobility models. For example, the average delay under RW model with constant step-length is almost 5 times worse than the analytical prediction based on the Poisson contact assumption. When $\mathbb{E}\{A_{\text{on}}\}$ (and also $\mathbb{E}\{A_{\text{off}}\}$) is relatively small (say, $\mathbb{E}\{A_{\text{on}}\} = 1$, the first point of x -axis), the impact of mobility still remains effective. However, as $\mathbb{E}\{A_{\text{on}}\}$ starts to increase, the measured average delays under all mobility models become almost identical to the analytical prediction (the ratio is close to one). This corresponds to the intermediate node-pair on/off dynamics, as expected from Theorem 2. Clearly, in this regime, the impact of mobility disappears and interestingly the usual Poisson contact assumption (now for the transfer opportunities) prevails. On the other hand, when $\mathbb{E}\{A_{\text{on}}\}$ is very large (say, $\mathbb{E}\{A_{\text{on}}\} = 32805$, the ending point of x -axis), then the measured delay performance is much different from the analytical prediction, implying that the user availability takes over in deciding network performance as also suggested in Section III-B (the slow on/off dynamics).

Figure 5(b) shows $\mathbb{P}\{L_{\text{off}} > t\}$ when $\mathbb{E}\{A_{\text{on}}\} = 45$ on a semi-log scale. The inter-transfer time distributions become very close to an exponential with the same mean, under all mobility choices, as expected from Theorem 2. When $\mathbb{E}\{A_{\text{on}}\} = 32805$, however, the inter-transfer time distributions highly deviate from the exponential and also depend on mobility models, as seen in Figure 5(c). We also test the hyper-exponentially distributed A_{off} , B_{off} and report the delay ratio in Figure 5(d). Again, we observe similar trend as in Figure 5(a), while the actual ratio values are slightly different from the case of exponentially distributed off duration for each node.

A map-based mobility model: We also consider a map-based mobility model included in the ONE simulator [21]. In this model, each mobile node chooses a random point on the map of Helsinki downtown area, shown Figure 6(a), and then follows the *shortest* route to that point from their current location under the geographical constraint of the area. The points are chosen completely randomly over the map (‘Random’ scenario) or from a list of prespecified points of interest representing popular places (‘POI’ scenario). For both scenarios, the initial node locations over the map are also chosen uniformly at random. As done for random walk models, we use the same node speed 1 m/s and Boolean model with range 20m for contact, with no pause time effect, and

[¶]To avoid any possible bias, we exclude the consecutive small samples of AB_{off} during the course of same contact duration T_C , in estimating $\mathbb{E}\{L_{\text{off}}\}$. Such situation arises when two nodes are in contact under the fast node-pair on/off dynamics, in which only the first L_{on} matters while all the many subsequent short-lived samples do not contribute toward any message transfer.

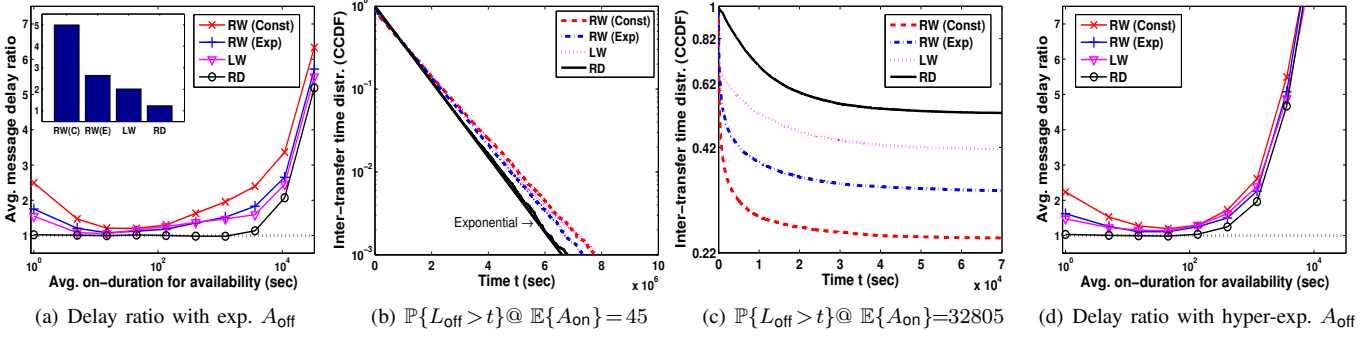


Fig. 5. Random walk models. (a) Delay ratio for the exponential off-duration A_{off} while varying $\mathbb{E}\{A_{\text{on}}\}$ (and also $\mathbb{E}\{A_{\text{off}}\}$); $\mathbb{P}\{L_{\text{off}} > t\}$ measured when (b) $\mathbb{E}\{A_{\text{on}}\} = 45$ and (c) $\mathbb{E}\{A_{\text{on}}\} = 32805$ (corresponding to third and last data points in the figure (a), respectively); (d) Delay ratio for the hyper-exp. A_{off} .

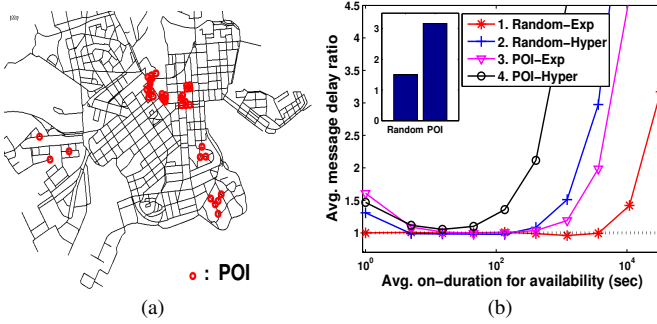


Fig. 6. A map-based mobility model. (a) Helsinki downtown area map with points of interest (red circles); (b) Delay ratio for ‘Random’ and ‘POI’ settings with exponential and hyper-exponential off-duration distributions.

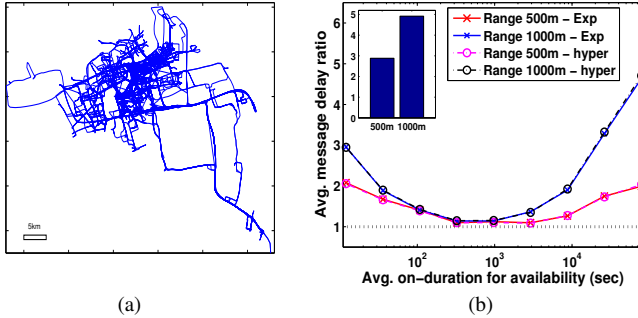


Fig. 7. GPS mobility traces. (a) Sample GPS traces of a Shanghai taxi; (a) Delay ratio with different transmission ranges $d = 500, 1000\text{m}$

then the same process for network performance comparison with 100 mobile nodes.

Figure 6(b) shows the delay ratio obtained under each scenario with different off-duration distributions. Again, the inset figure shows the ratio with always-on mobile nodes for communication. Similar to the case of random walk models, we can see that the impact of mobility is first effective and then becomes vanishingly small for the mid-range of $\mathbb{E}\{A_{\text{on}}\}$ (and so for $\mathbb{E}\{A_{\text{off}}\}$), while the user availability eventually takes over as the time scale for on/off dynamics gets larger (slow dynamics). We also observe that the impact of slow on/off dynamics is more striking in ‘POI’ than ‘Random’ scenario.

GPS mobility traces: We finally validate our findings through GPS traces-driven simulation. To this end, we use the GPS traces of around 4000 Shanghai taxis [1], by far, the largest GPS traces publicly available with high granularity. The location information of each taxi is recorded every 1–3 minutes

within a Shanghai area of around $191 \times 224 \text{ km}^2$ for 28 days. Figure 7(a) depicts sample GPS traces of a taxi. For performance evaluation, we first conduct interpolation to obtain the location information of each taxi every 1 minute, compute the total travel distance for each taxi, and choose top 100 taxis. We also use the Boolean model for contact with transmission range $d = 500, 1000\text{m}$. This is because we need enough contact samples among taxis (nodes) to correctly evaluate the impact of node on/off availability process. For comparison under each setting of the on/off process, we numerically generate a series of Poisson transfer opportunities for each node pair with the empirical average inter-transfer time, run the epidemic routing protocol, and measure average delay to be used as a baseline. Figure 7(b) shows the delay ratio (to the baseline) under each choice of the transmission ranges with different off-duration distributions, where the inset figure shows the ratio with always-on nodes for communication. There is not much difference between different off-duration distributions. This is largely due to the fact that we have only one instance of contact/inter-contact samples, as opposed to synthetic models so far for which we can repeatedly generate different mobility samples to get reliable estimates. Nonetheless, Figure 7(b) again reveals the similar trend as in the random walk models and map-based mobility model.

V. DISCUSSION AND CONCLUSION

Our findings have indicated that mobility alone – even with fine-grained GPS-coordinates for every user, is not sufficient to fully characterize the link-level dynamics and there exists another equally important and orthogonal dimension, namely, *user availability* for communication, which has been largely overlooked in the literature. Specifically, we have identified the presence of three different regimes depending on the relative time scale between user availability and mobility-induced contact/inter-contact processes, as summarized in Figure 8(a). In particular, the user availability dynamics alone can drive the link-level dynamics and its resulting network performance into many other ways possible, which are completely different from the prediction when only the mobility (or contact/inter-contact dynamics) is taken into account.

To gauge how much the user availability process can affect the link-level dynamics, recall the link formation process $\mathbf{1}_{\{L(A-B)\}}(t) = \mathbf{1}_{\{B(t) \in \mathcal{C}_A(t)\}} \cdot I_A(t) \cdot I_B(t)$ in (4). On the

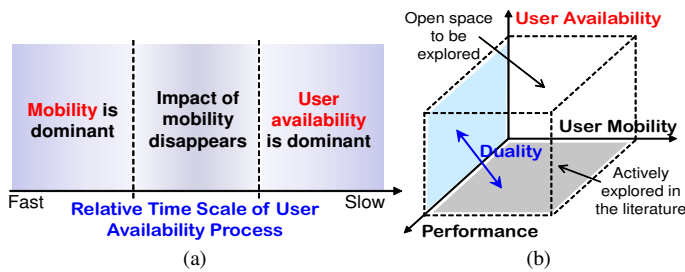


Fig. 8. (a) Three different regimes depending on the relative time scale of user availability process; (b) The role of user availability.

one hand, if all mobile nodes are always ‘on’ for communication, as commonly considered in the current literature, then $\mathbf{1}_{\{L(A-B)\}}(t) = \mathbf{1}_{\{B(t) \in C_A(t)\}}$ and so the mobility-induced contact/inter-contact process fully characterizes the link-level dynamics. On the other hand, if all mobile nodes are always in ‘contact’ with each other, then $\mathbf{1}_{\{L(A-B)\}}(t) = I_A(t)I_B(t)$, implying that the user availability process is now the sole factor. Indeed, the link formation process is simply the product of $\mathbf{1}_{\{B(t) \in C_A(t)\}}$ and $I_A(t)I_B(t)$, with equal and indistinguishable contribution from each of these 0–1 processes. That is, the mobility-induced contact/inter-contact dynamics and the user-pair availability can be thought of as ‘dual’ of each other. See Figure 8(b) for illustration. Thus, the currently prevalent arguments centered around power-law or dichotomic inter-contact time distribution, mainly obtained in the former case, can also be *equally applicable* for the latter case. Clearly, the impact of user availability can be significant to the same extent as that of user mobility.

While mobility-related research studies abound in the literature, most of them assumed the wireless interfaces of mobile nodes to be always ‘on’ and dedicated for communication. However, as mentioned before, when it comes to reality with mobile devices carried by humans, a number of constraints including limited battery power prevent the wireless interface of each user from being always on, and make the common assumption questionable.^{||} More importantly, our findings caution that such an assumption can lead to largely misleading results, but at the same time, suggest that there exist many uncharted territories for further exploration, as depicted in Figure 8(b). We envision that our findings stimulate active research on more in-depth studies of user availability and its impact on network performance. It can be also possible to analyze the *joint* impact of user mobility and availability on the scaling properties of network capacity and delay.

REFERENCES

- [1] “Wireless and Sensor networks Lab (WnSN), Shanghai Jiao Tong University,” <http://wirelesslab.sjtu.edu.cn/>.
- [2] “PCWorld, why your smartphone battery sucks,” May 2011, http://www.pcworld.com/article/228189/why_your_smartphone_battery_sucks.html.
- [3] E. Altman, G. Neglia, F. De Pellegrini, and D. Miorandi, “Decentralized stochastic control of delay tolerant networks,” in *IEEE INFOCOM*, 2009.

^{||}The low chance of ‘true’ transfer opportunities, for the performance of opportunistic mobile networking, can be compensated by the large node populations carrying mobile devices – the power of the crowd [38], although the design of actual system architecture and its performance are clearly beyond the scope of our paper.

- [4] F. Baccelli and P. Brémaud, *Elements of queueing theory: Palm martingale calculus and stochastic recurrences*. Springer-Verlag, 2003.
- [5] A. Balasubramanian, B. N. Levine, and A. Venkataramani, “DTN routing as a resource allocation problem,” in *ACM Sigcomm*, 2007.
- [6] N. Banerjee, M. D. Corner, D. Towsley, and B. N. Levine, “Relays, base stations, and meshes: enhancing mobile networks with infrastructure,” in *ACM MobiCom*, 2008.
- [7] J. A. Bitsch Link, C. Wollgarten, S. Schupp, and K. Wehrle, “Perfect difference sets for neighbor discovery: energy efficient and fair,” in *ExtremeCom*, 2011.
- [8] M. Brown, “Approximating IMRL distributions by exponential distributions, with applications to first passage times,” *Annals of Probability*, vol. 11, no. 2, pp. 419–427, May 1983.
- [9] H. Cai and D. Y. Eun, “Crossing over the bounded domain: from exponential to power-law inter-meeting time in MANET,” in *ACM MobiCom*, 2007.
- [10] —, “Toward stochastic anatomy of inter-meeting time distribution under general mobility models,” in *ACM MobiHoc*, 2008.
- [11] A. Chaintreau, P. Hui, J. Crowcroft, C. Diot, R. Gass, and J. Scott, “Impact of human mobility on the design of opportunistic forwarding algorithms,” in *IEEE INFOCOM*, 2006.
- [12] A. Chaintreau, J.-Y. Le Boudec, and N. Ristanovic, “The age of gossip: spatial mean field regime,” in *ACM SIGMETRICS/Performance*, 2009.
- [13] V. Conan, J. Leguay, and T. Friedman, “Characterizing pairwise inter-contact patterns in delay tolerant networks,” in *Autonomics*, 2007.
- [14] A. Feldmann and W. Whitt, “Fitting mixtures of exponentials to long-tail distributions to analyze network performance models,” in *IEEE INFOCOM*, 1997.
- [15] W. Feller, *An introduction to probability theory and its applications*. John Wiley & Son, 1968.
- [16] R. Groeneveld, G. Koole, and P. Nain, “Message delay in mobile ad hoc networks,” in *Performance*, 2005.
- [17] B. Han, P. Hui, V. S. A. Kumar, M. V. Marche, G. Pei, and A. Srinivasan, “Cellular traffic offloading through opportunistic communications: a case study,” in *CHANTS*, 2010.
- [18] P. Hui, J. Crowcroft, and E. Yoneki, “BUBBLE Rap: social-based forwarding in delay tolerant networks,” in *ACM MobiHoc*, 2008.
- [19] S. Ioannidis, A. Chaintreau, and L. Massoulie, “Optimal and scalable distribution of content updates over a mobile social network,” in *IEEE INFOCOM*, 2009.
- [20] T. Karagiannis, J.-Y. Le Boudec, and M. Vojnovic, “Power law and exponential decay of inter contact times between mobile devices,” in *ACM MobiCom*, 2007.
- [21] A. Keränen, J. Ott, and T. Kaikkänen, “The ONE simulator for DTN protocol evaluation,” in *SIMUtools*, 2009.
- [22] S. Kim, C.-H. Lee, and D. Y. Eun, “Super-diffusive behavior of mobile nodes and its impact on routing protocol performance,” *IEEE Trans. on Mobile Computing*, vol. 9, no. 2, pp. 288–304, Feb. 2010.
- [23] P. Kuusela, I. Norros, and P. Raatikainen, “Report on modeling reliability of an IP network and strategies for improving the reliability,” VTT, Technical Research Center of Finland, Tech. Rep., June 2009.
- [24] K. Lee, S. Hong, S. J. Kim, I. Rhee, and S. Chong, “SLAW: a new mobility model for human walks,” in *IEEE INFOCOM*, 2009.
- [25] U. Lee, S. Y. Oh, K.-W. Lee, and M. Gerla, “Scaling properties of delay tolerant networks with correlated motion patterns,” in *CHANTS*, 2009.
- [26] J. Manweiler and R. R. Choudhury, “Avoiding the rush hours: WiFi energy management via traffic isolation,” in *ACM MobiSys*, 2011.
- [27] A. Mei and J. Stefa, “SWIM: a simple model to generate small mobile worlds,” in *IEEE INFOCOM*, 2009.
- [28] M. Motani, V. Srinivasan, and P. S. Nuggehalli, “PeopleNet: Engineering a wireless virtual social network,” in *ACM MobiCom*, 2005.
- [29] A.-K. Pietiläinen and C. Diot, “Experimenting with opportunistic networking,” in *ACM MobiArch*, 2009.
- [30] A.-K. Pietiläinen, E. Oliver, J. LeBrun, G. Varghese, and C. Diot, “MobiClique: Middleware for mobile social networking,” in *WOSN*, 2009.
- [31] S. M. Ross, *Stochastic processes*, 2nd ed. John Wiley & Son, 1996.
- [32] J. G. Shanthikumar, “DFR property of first-passage times and its preservation under geometric compounding,” *Annals of Probability*, vol. 16, no. 1, pp. 397–406, Jan. 1988.
- [33] T. Spyropoulos, K. Psounis, and C. S. Raghavendra, “Efficient routing in intermittently connected mobile networks: the multiple-copy case,” *IEEE/ACM Trans. on Networking*, vol. 16, no. 1, pp. 77–90, Feb. 2008.
- [34] A. Vahdat and D. Becker, “Epidemic routing for partially-connected ad hoc networks,” Duke University, Tech. Rep., April 2000.
- [35] V. Vukadinović and G. Karlsson, “Spectral efficiency of mobility-assisted podcasting in cellular networks,” in *MobiOpp*, 2010.
- [36] W. Wang, V. Srinivasan, and M. Motani, “Adaptive contact probing mechanisms for delay tolerant applications,” in *ACM MobiCom*, 2007.
- [37] X. Zhang, G. Neglia, J. Kurose, and D. Towsley, “Performance modeling of epidemic routing,” *Computer Networks*, vol. 51, no. 10, pp. 2867–2891, 2007.
- [38] G. Zyba, G. M. Voelker, S. Ioannidis, and C. Diot, “Dissemination in opportunistic mobile ad-hoc networks: the power of the crowd,” in *IEEE INFOCOM*, 2011.